THE JOURNAL OF PHYSICAL CHEMISTRY A

ARTICLE

pubs.acs.org/JPCA

Interaction between Nuclear Graphite and Molten Fluoride Salts: A Synchrotron Radiation Study of the Substitution of Graphitic Hydrogen by Fluoride Ion

Xinmei Yang,[†,‡] Shanglei Feng,[†,‡] Xingtai Zhou,[*,†,‡] Hongjie Xu,[*,†,‡] and T. K. Sham[*,§]

[†]Shanghai Synchrotron Radiation Facility, Shanghai, 201204 China

[‡]Key Laboratory of Nuclear Analysis Technique (Shanghai), Shanghai Institute of Applied Physics, Chinese Academy of Sciences, Shanghai, 201800 China

[§]Department of Chemistry, The University of Western Ontario, London, Ontario, N6A 5B7, Canada

ABSTRACT: The interaction between nuclear graphite and molten fluoride salts (46.5 mol % LiF/11.5 mol % NaF/42 mol % KF) is investigated by synchrotron X-ray diffraction and C K-edge X-ray absorption near-edge structure (XANES). It is found that there are a large number of H atoms in IG-110 nuclear graphite, which is attributed to the residual C−H bond after the graphitization process of petroleum coke and pitch binder. The elastic recoil detection analysis indicates that H atoms are uniformly distributed in IG-110 nuclear graphite, in excellent agreement with the XANES results. The XANES results indicate that the immersion in molten fluoride salts at 500 °C led to H atoms in nuclear graphite partly substituted by the fluorine from fluoride salts to form C−F bond. The implications of these findings are discussed.

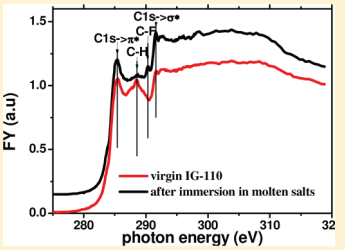

I. INTRODUCTION

Graphite, which can be used to slow down fast neutrons produced by nuclear reaction, has been used as a neutron moderator in many reactors, such as a molten salt reactor system (MSR). MSR is one of six reactor systems (gas-cooled fast reactor system, lead-cooled fast reactor system, molten salt reactor system, sodium-cooled fast reactor system, supercritical-water-cooled reactor system, and very-high-temperature reactor system) proposed by the Generation IV International Forum.[1] Different from most reactors in which solid fuel is used, a mixture of circulating liquid fluoride salts is used as fuel in the MSR system. The fuel in MSR is a mixture of molten carrier salts and fuel salts (uranium fluoride and thorium fluoride),[1,2] which flow through graphite moderator channels during the operation of a MSR reactor. The compatibility of nuclear graphite with fresh molten salts is one of technology gaps for MSR.[1] A large number of experiments in the literature indicate that graphite can react with fluorine and relatively oxidizing fluorine compounds, such as ClF_3, BrF_3, XeF_2, and LiF, to form graphite fluoride $(CF_x)_n$,[3−22] where $0 < x \leq 1.25$. It should be noted that although the reaction of benzene with NaF to form monofluorobenzene is thermodynamically highly unlikely, our experiments used mixed fluoride ionic liquids. Thus, the conditions for the formation of C−F are more favorable when nuclear graphite is immerged in a hot ionic liquid of mixed fluorides.

Figures 1 and 4 in ref 4 present a structure model for graphite fluoride, showing that the C−F bond is not in the basal plane of the graphite sheet,[9,23−28] and fluorine preferentially bonds to the next neighbor carbon atoms in the basal plane on the other side. Therefore, the lattice of graphite is expanded by forming a C−F bond during fluorination.[8,9,13,17,25,29,30] The fluorination of graphite is dependent on the duration, temperature, and pressure of fluorination and the size of crystallite.[7,9,31] The petroleum coke, which is graphitized from green coke at 2100−2700 °C, can also react with fluorine to form $(CF)_n$, $(C_2F)_n$, or their mixture.[7] The nuclear graphite in our studies is IG-110 grade, which is graphitized from petroleum coke and pitch binder.[32] Therefore, there is a possibility for nuclear graphite to react with fluorine to form $(CF_x)_n$; however, most previous works have not focused on the interaction between graphite and the molten fluoride salts. Furthermore, for nuclear graphite, C−H bonds are partly residual after the graphitization of raw materials. The H atoms bonded to the C atoms at the edge of graphite can be replaced with F atoms.[33−35] Because the dissociation energy of C−F bond is higher than that of the C−H bond,[36] the C−F bond in graphite is more stable than the C−H bond. Therefore, a C−F bond can form by the reaction between nuclear graphite and molten fluorine salts, which will result in the expansion of the graphite lattice and affect the performance of nuclear graphite in MSR.

In this study, we investigated the interaction between nuclear graphite and molten salt (a mixture of 46.5 mol % LiF/11.5 mol % NaF/42 mol % KF). The molten salts used in our experiments exhibit melting points similar to a mixture of 67 mol % LiF/33 mol % BeF_2 and a mixture of 64.5 mol % LiF/30.5 mol % BeF_2/5 mol % ZrF_4,[37] which can be the candidate for molten salt coolants. In this study, the commercially available IG-110 nuclear graphite from Toyo Tanso Co. Ltd. was used. This material has been used as the neutron moderator for a high-temperature engineering test reactor in Japan and a high-temperature gas-cooled reactor in China.[38] We employed elastic recoil detection

Received: September 17, 2011
Revised: December 13, 2011
Published: January 17, 2012

(ERD) analysis to detect H atoms and to study its distribution in nuclear graphite. We also employed synchrotron X-ray diffraction (XRD) and C K-edge X-ray absorption near-edge structure (XANES) to study the structure and the chemical state of nuclear graphite at room temperature before and after immersion in molten fluoride salts.

II. EXPERIMENTAL SECTION

The material used in the present study is IG-110 nuclear graphite from Toyo Tanso Co. Ltd., which is made of petroleum coke and pitch binder and produced by an isostatic molding method.[47] The average grain size in IG-110 graphite is ~20 μm.[47,55] There are micropores with a mean diameter of >1 μm in the graphite.[55] Samples used in this study are cut from bulk IG-110 nuclear graphite, having a dimension of 5 × 5 × 2 mm^3. The samples were washed in alcohol and acetone and then in distilled water under ultrasonic bath to clean the surface; after that, they were heated at 500 °C for 4 h under high vacuum (10^{-5} Pa) to eliminate possible adsorption. The samples were then immerged in molten salt to investigate the interaction between nuclear graphite and molten fluoride salts. The molten salt was synthesized from commercial fluoride salts with a composition of 46.5 mol % LiF (99.9% purity, from Aladdin Chemistry Co. Ltd.), 11.5 mol % NaF (99% purity, from Aladdin Chemistry Co. Ltd.) and 42 mol % KF (99% min purity, from Acros Organics), which is the candidate for coolant in a MSR reactor and advanced high-temperature reactor because of its low melting point (454 °C), high heat capacity, and its high chemical stability at high temperature.[37,56]

Graphite samples and fluoride salts were introduced in a closed nickel crucible and heated in a furnace at 500 °C for 16 h. The furnace was pumped out with a mechanical pump to prevent air, where the pressure was ~10^2 Pa because of the saturation vapor pressure of molten fluoride salts.

The samples before and after immersion in molten salts were characterized by synchrotron XRD (λ = 1.2438 Å) and XANES. The room temperature XRD measurements were performed at the BL14B beamline of the Shanghai Synchrotron Radiation Facility (SSRF). The diffraction range is $6° < 2\theta < 76°$, with a step size $\Delta 2\theta = 0.02°$ and a counting time of 1s per step. The XANES spectra at the C K-edge were performed at the spherical grating monochromator (SGM) undulator beamline at Canada Light Source (CLS), a 2.9GeV, third-generation synchrotron facility located in Saskatoon.[57] The energy resolution ($\Delta E/E$) of SGM beamline in CLS is ~2×10^{-4} over the photon energy range from 250 to 1500 eV. XANES spectra were recorded simultaneously in total electron yield (TEY) and X-ray fluorescence yield (FY), using specimen current and a multichannel plate detector, respectively. TEY and FY measurement provides surface and bulk sensitivity, respectively, albeit the latter was sometimes obscured by the thickness effect (self-absorption, leading to broadening of intense resonance). The XANES spectra were normalized to the incidence photon flux, I_o, recorded using a Au mesh, which was refreshed by Au evaporation prior to the measurement. The ERD analysis, which is used to detect H atoms and to study the distribution of H atoms in graphite samples, is performed in a 4 MeV static electricity accelerator using a 3 MeV $^4He^+$ ion beam with an irradiation area 3 mm in diameter.

III. RESULTS AND DISCUSSIONS

Figure 1a displays the XRD pattern of virgin IG-110 nuclear graphite, showing that the graphite phase is mainly hexagonal

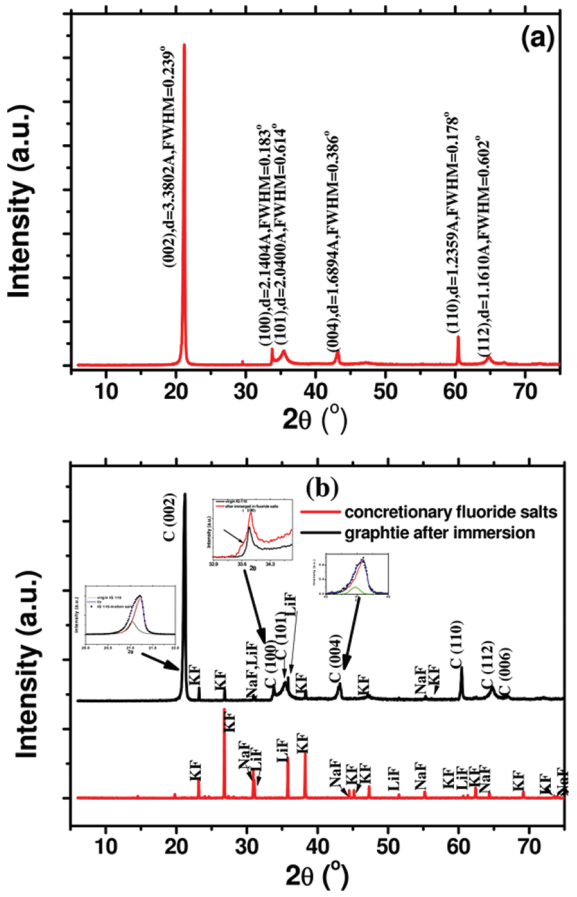

Figure 1. XRD pattern of IG-110 nuclear graphite: (a) the virgin IG-110 nuclear graphite and (b) after immersion in molten fluoride salts (blue line). The black line in panel b is the XRD pattern of the concretionary fluoride salts.

(graphtie-2H: hexagonal, $a = b$ = 2.463 Å, c = 6.714 Å, U = 35.27 Å, space group $P63/mmc\{P63/m2/m2/c\}$, Z = 4). Figure 1b presents an XRD pattern of concretionary fluoride salts (black line) and that of IG-110 nuclear graphite after immersion in molten fluoride salts (blue line), showing that there are LiF, NaF, KF, and graphite-2H phases in IG-110 nuclear graphite after immersion, indicating that fluoride salts can immerge into the surface micropores in IG-110 nuclear graphite.

The diffraction peaks in Figure 1b are broader than their corresponding counterparts in Figure 1a. The (002) peak of the graphite phase in Figure 1b can be fitted well with two Gaussian lines (insert of Figure 1b). One Gaussian line is 92.6% times the unitary (002) peak of virgin IG-110 nuclear graphite in Figure 1a. The other is a Gaussian line with a lower 2θ, indicating that the interlayer spacing of IG-110 nuclear graphite is increased after immersion in fluoride salts, which is associated with the formation of the C−F bond. The (004) peak of the graphite phase in Figure 1b has similar character. Previous results indicate that the interlayer spacing of graphite increases upon fluorination.[8,9] The broadening of the diffraction peak and the appearance of a shoulder at a lower diffraction angle after immersion in fluoride salts are also evident in the evolution of the (100) peak of IG-110 nuclear graphite, which is consistent with previous results for the expansion of graphite after fluorination.[8,9,13,17,25,29,30] Therefore, it is entirely conceivable that C−F bonds will form in IG-110

dx.doi.org/10.1021/jp208990y |J. Phys. Chem. A 2012, 116, 985–989

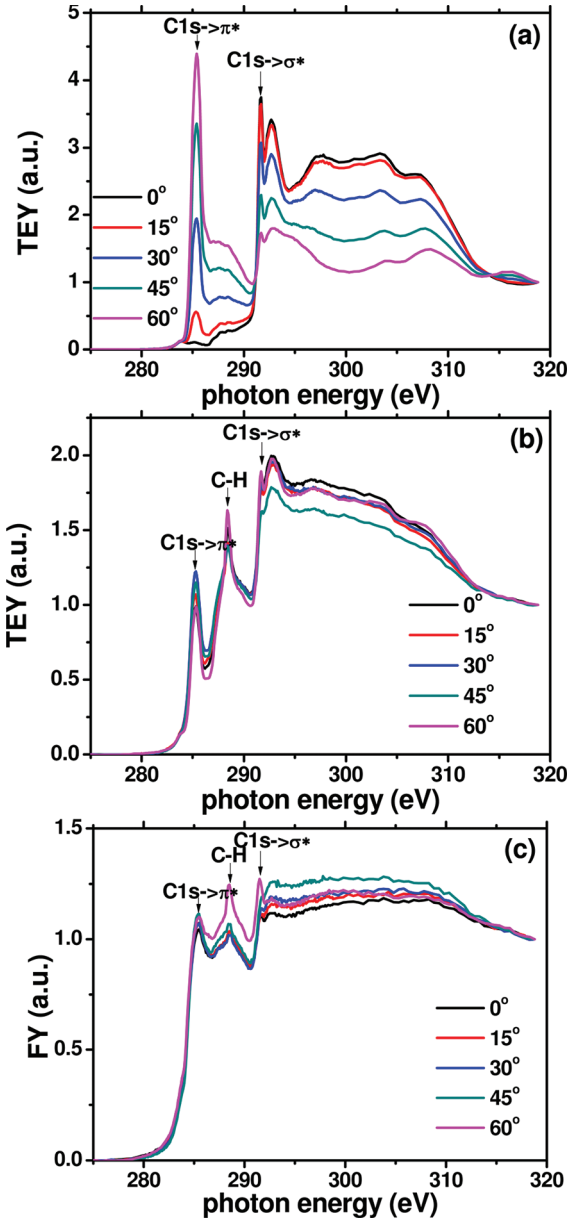

Figure 2. The C K-edge XANES spectra at room temperature: (a) the TEY spectra of HOPG, (b) the TEY spectra of IG-110 nuclear graphite, and (c) the FY spectra of IG-110 nuclear graphite.

nuclear graphite after immersion in molten fluoride salts. The following experiments employed with C K-edge XANES indicate that a C−F bond is, indeed, forming in IG-110 nuclear graphite after immersion in molten fluoride salts.

Figure 2 shows the angle-dependent C K-edge XANES spectra, measured at room temperature. The quoted angle (henceforth denoted α) in Figure 2 describes the angle between the sample surface and X-ray polarization vector; for example, $\alpha = 0°$ means normal incidence of the linearly polarized light. In this configuration, the polarization vector lies in the basal plane and is perpendicular to the orientation of π^* states in graphite.[39,40] A uniform background signal extrapolated from the monotonic signal below edge has been removed, and the spectra were normalized to unity at 320 eV.

Figure 2a is the angle-dependent C K-edge XANES spectra of a reference compound, the highly oriented pyrolytic graphite

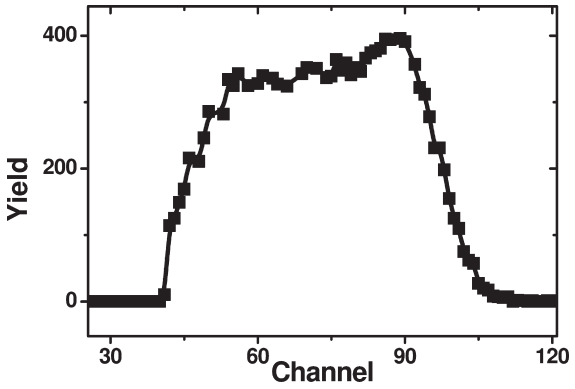

Figure 3. ERD spectra of IG-110 graphite, measured with 3.0 MeV $^4He^+$ beam.

(HOPG), recorded in TEY. The peak centered at ∼285.4 eV is assigned to the C 1s electron transition to an unoccupied π^* orbital ($C_{1s\rightarrow\pi^*}$).[41−43] The peak at 291.7 eV is assigned to the C 1s electron transition to an unoccupied σ^* orbital ($C_{1s\rightarrow\sigma^*}$).[41−43] Figure 2a shows that the intensity of the $C_{1s\rightarrow\pi^*}$ transition increases with increasing α, angle between sample surface and X-ray polarization, which indicates that the π^* orbital is perpendicular to the *ab* plane (cos 90 = 0), as expected. The evolution of the $C_{1s\rightarrow\sigma^*}$ transition intensity with the quoted angle, α, is inversely correlated with that of the $C_{1s\rightarrow\pi^*}$ transition, which indicates that the σ^* orbital is parallel to the *ab* plane. The transition probability is proportional to the transition matrix element described by $|\langle 1s|\cos\alpha|f\rangle|^2$, where 1*s* is the initial state wave function and *f* is the final state wave function; for example, π^* or σ^*, and cos α is the angular part of matrix element following dipole selection rules. Thus, the C K-edge probes the occupancy and symmetry of unoccupied densities of states of C 2p character in the vicinity of threshold. The observed angle-dependent intensity variation of the $C_{1s\rightarrow\pi^*}$ and $C_{1s\rightarrow\sigma^*}$ transition indicates that HOPG is anisotropic,[41,42] as its name suggests.

Figure 2b is the C K-edge XANES spectra of virgin isotropic graphite recorded in TEY, showing that there are three peaks centered at ∼285.3, ∼288.4, and ∼291.7 eV, with no significant angular dependence. The peaks centered at ∼285.3 and ∼291.7 eV are assigned to the C 1s electron transition to the unoccupied π^* orbital and the σ^* orbital, respectively, which indicates that the microcrystal in IG-110 nuclear graphite is well graphitized with random orientation. The peak centered at ∼288.4 eV has a slight inverse dependence of the quoted angle α compared with the π^* orbital, revealing that the structure corresponding to ∼288.4 eV is in the *ab* plane of the graphite. The peak centered at ∼288.4 eV is very sharp and is assigned to the σ^*_{C-H} transition of the C−H bond,[41,44−46] which is attributed to a large amount of residual hydrogen after graphitization of raw materials used in the manufacture of isotropic graphite. The IG-110 nuclear graphite used in our experiments is made of petroleum coke and pitch binder and produced by an isostatic molding method.

The peak centered at ∼288.4 eV is also evident in more bulk sensitive FY spectra (Figure 2c), despite some broadening due to self-absorption, indicating that the C−H bond is not only at the surface of nuclear graphite but also throughout the specimen. The conclusion of the presence of H atoms in the IG-110 nuclear graphite is consistent with the result of the ERD spectrum of the IG-110 nuclear graphite shown in Figure 3. The ERD spectrum indicates that H atoms are almost uniformly distributed in graphite.

dx.doi.org/10.1021/jp208990y |*J. Phys. Chem. A* 2012, 116, 985–989

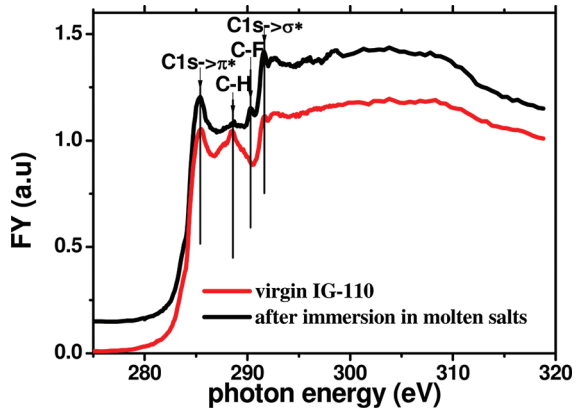

Figure 4. The C K-edge XANES spectrum in FY of isotropic graphite before (red line) and after (black line) immersion in molten fluoride salt for 16 h, measured at room temperature.

Therefore, the C−H bond is intrinsic to IG-110 nuclear graphite and cannot be attributed to the absorption of $C_xH_yO_z$ compounds. The slight angle dependence of peaks centered at ~285.3, ~291.7 eV indicates that the structure of the IG-110 nuclear graphite is close to isotropic, which is attributed to the random distribution of graphite microcrystals in the specimen.

It has been reported that graphite microcrystals with an average grain size of ~20 μm[47] are randomly distributed, although some texture may exist because the material is more sheetlike than spherical. IG-110 nuclear graphite has an isotropic ratio below 1.05,[48] the ratio of thermal expansion parallel to the sample surface to that perpendicular to the sample surface. The IG-110 nuclear graphite has almost isotropic neutron irradiation-induced dimensional changes that can be up to 3.6×10^{22} n/cm^2 (E > 0.1 MeV) at an irradiation temperature of 600 °C.[49] Therefore, the IG-110 nuclear graphite is one of the nuclear graphite candidates for the generation IV nuclear reactors.[47]

Figure 4 displays the C K-edge XANES spectrum in FY of IG-110 nuclear graphite after immersion in molten fluoride salt at 500 °C for 16 h, showing the chemical structure evolution of IG-110 nuclear graphite induced by immersion. In addition to the peaks at ~285.4, ~291.6, and ~288.5 eV, an additional peak centered at ~290.3 eV can be observed. We attributed this peak at ~290.3 eV to the σ^*_{C-F} transition of the C−F bond.[33,50−54] By comparing with the FY spectra in Figure 2c, we find that the peak centered at ~290.3 eV emerges at the expense of a C−H bond, corresponding to the decreasing peak centered at ~288.5 eV. These results indicate that the fluorine anions from molten fluoride salts can substitute for the H atoms and form C−F bonds. Thus, the C−F bond can be generated by fluorination involving negatively charged fluoride ions in a molten salt. A larger variety of fluoride salts can release fluoride anions in graphite to form C−F bonds. The ═C−F bonds can also come into being in a HOPG sample by F^+ ion irradiation.[22]

IV. CONCLUSIONS

We have employed synchrotron XRD, C K-edge XANES, and ERD analysis to investigate the interaction between IG-110 nuclear graphite and fluoride salts (46.5 mol % LiF, 11.5 mol % NaF, and 42 mol % KF). It is found that after the immersion of nuclear graphite in molten fluoride salts, some fluoride salts can immerge into the micropores of the IG 110 nuclear graphite. The H atoms uniformly distributed in nuclear graphite in the form of graphitic C−H bonds are partly replaced with fluorine, which reacts with nuclear graphite and form C−F bonds.

AUTHOR INFORMATION

Corresponding Author

*Phone: +86-21-5955477. Fax: +86-21-59552539. E-mail: zhouxingtai@sinap.ac.cn (X.Z.), xuhongjie@sinap.ac.cn (H.X.), sham@uwo.ca (T.K.S.).

ACKNOWLEDGMENT

We are grateful for the XRD measurements at the BL14B beamline of SSRF and C K-edge XANES spectrum measurements at SGM beamline of CLS and technical assistance of Tom Regier and David Chevrier. The research work at Shanghai Institute of Applied Physics was supported by the Major State Basic Research Development Program of China (National Project 973) under Grant no. 2010CB934500, Stratagemically Leading Program of the Chinese Academy of Science under Grant no. XDA020407400, and the 100 Talents Program of the Chinese Academy of Science and Outstanding Returned Student Program of the Department of Human Resources and Social Security. The research at the University of Western Ontario was supported by NSERC, CFI, CRC, and OIT. Canadian Light Source is supported by NSERC, NRC, CIHR, and the University of Saskatchewan.

REFERENCES

(1) *A Technology Roadmap for Generation IV Nuclear Energy Systems*; Report USDOE/GIG-002-00; The U.S. DOE Nuclear Research Advisory Committee and the Generation IV International Forum, 2002.

(2) Rosenthal, M. W.; Haubenreich, P. N.; Briggs, R. B. *The Development Status of Molten-Salt Breeder Reactors*; Report ORNL-4812; National Technical Information Service: Springfield, Virginia, United States of America, 1972.

(3) Hamwi, A.; Daoud, M.; Cousseins, J. C. *Synth. Met.* **1988**, *26*, 89–98.

(4) Hamwi, A. *J. Phys. Chem. Solids* **1996**, *57*, 677–688.

(5) Gnérin, K.; Pinheiro, J. P.; Dubois, M.; Fawal, Z.; Masin, F.; Yazami, R.; Hamwi, A. *Chem. Mater.* **2004**, *16*, 1786–1793.

(6) Delabarre, C.; Guérin, K.; Dubois, M.; Giraudet, J.; Fawal, Z.; Hamwi, A. *J. Fluorine Chem.* **2005**, *126*, 1078–1087.

(7) Watanabe, N.; Nakajima, T. *Graphite Fluorides and Carbon-Fluorine Compounds*; CRC Press: Boca Raton, 1991.

(8) Nazarov, A. S.; Makotchenko, V. G.; Fedorov, V. E. *Inorg. Mater.* **2006**, *42*, 1260–1264.

(9) Kita, Y.; Watanabe, N.; Fujii, Y. *J. Am. Chem. Soc.* **1979**, *101*, 3832–3841.

(10) Giraudet, J.; Dubois, M.; Guérin, K.; Delabarre, C.; Hamwi, A.; Masin, F. *J. Phys. Chem. B* **2007**, *111*, 14143–14151.

(11) Dubois, M.; Gnérin, K.; Pinheriro, J. P.; Masin, F.; Fawal, Z.; Hamwi, A. *Carbon* **2004**, *42*, 1931–1940.

(12) Gnérin, K.; Pinheriro, J. P.; Dubois, M.; Fawal, Z.; Masin, F.; Yazami, R.; Hamwi, A. *Chem. Mater.* **2004**, *16*, 1786–1792.

(13) Sato, Y.; Itoh, K.; Hagiwara, R.; Fukunaga, T.; Ito, Y. *Carbon* **2004**, *42*, 3243–3249.

(14) Mallouk, T.; Bartlett, N. *J. Chem. Soc., Chem. Commun.* **1983**, *1013*, 103–105.

(15) Nakajima, T.; Watanabe, N.; Kameda, I.; Endo, M. *Carbon* **1986**, *24*, 343–351.

(16) Panich, A. M. *Synth. Met.* **1999**, *100*, 169–185.

(17) Touhara, H.; Kadono, K.; Fujii, Y.; Watanabe, N. *Anorg. Allg. Chem.* **1987**, *544*, 7–20.

(18) Watanabe, N. *Physica B+C* **1981**, *105*, 17–21.
(19) Lagow, R. J.; Badachhape, R. B.; Wood, J. L.; Margrave, J. L. *J. Chem. Soc., Dalton Trans.* **1974**, *12*, 1268–1273.
(20) Nakajima, T. *Fluorine—Carbon and Fluoride—Carbon Materials: Chemistry, Physics, and Application*; Marcel Dekker, Inc.: New York, 1995.
(21) Blöchl, P. E. *Phys. Rev. B* **1994**, *50*, 17953–17979.
(22) Sekiguchi, T.; Baba, Y.; Shimoyama, I.; Nath, K. G. *Surf. Interface Anal.* **2006**, *38*, 352–356.
(23) Watanabe, N.; Nakajima, T.; Tauhara, H. *Carbon Materials. Graphite Fluorides*; Elsevier: Amsterdam, 1988.
(24) Zhang, W.; Dubois, M.; Guérin, K.; Bonnet, P.; Kharbache, H.; Masin, F.; Kharitonov, A. P.; Hamwi, A. *Phys. Chem. Chem. Phys.* **2010**, *12*, 1388–1398.
(25) Ribas, M. A.; Singh, A. K.; Sorokin, P. B.; Yakobson, B. I. *Nano Res.* **2011**, *4*, 143–152.
(26) Zhou, J.; Wu, M. M.; Zhou, X.; Sun, Q. *Appl. Phys. Lett.* **2009**, *95*, 103108/1–3.
(27) Zhou, J.; Liang, Q.; Dong, J. *Carbon* **2010**, *48*, 1405–1409.
(28) Okotrub, A. V.; Asanov, I. P.; Yudanov, N. F.; Babin, K. S.; Gusel'nikov, A. V.; Nedoseikina, T. I.; Gevko, P. N.; Bulusheva, L. G.; Osváth, Z.; Biró, L. P. *Phys. Status Solidi B* **2009**, *246*, 2454–2548.
(29) Meshri, D. T. *Polymer News* **1980**, *6*, 200–207.
(30) Palin, D. E.; Wadsworth, K. D. *Nature* **1948**, *162*, 925–926.
(31) Delabarre, C.; Dubois, M.; Giraudet, J.; Guérin, K.; Hamwi, A. *Carbon* **2006**, *44*, 2543–2548.
(32) Kim, E.; Kim, Y. *Solid State Commun.* **2010**, *150*, 1633–1636.
(33) Jeon, K.; Lee, Z.; Pollak, E.; Moreschini, L.; Bostwick, A.; Park, C.; Mendelsberg, R.; Radmilovic, V.; Kostecki, R.; Richardson, T. J.; Rotenberg, E. *ACS Nano* **2011**, *5*, 1042–1046.
(34) Stabel, A.; Dasaradhi, L.; O'Hagan, D.; Rade, J. P. *Langmuir* **1955**, *11*, 1427–1430.
(35) Zboril, R.; Karlický, F.; Bourlinos, A. B.; Steriotis, T. A.; Stubos, A. K.; Georgakilas, V.; Safáfrová, K.; Jancík, D.; Trapalis, C.; Otyepka, M. *Small* **2010**, *6*, 2885–2891.
(36) O' Hagan, D. *Chem. Soc. Rev.* **2008**, *37*, 308–319.
(37) Williams, D. F.; Toth, L. M.; Clarno, K. T. *Assessment of Candidate Molten Salt Coolants for the Advanced High-Temperature Reactor (AHTR)*; Report ORNL/TM-2006/12; National Technical Information Service: Springfield, Virginia, United States of America, 2006.
(38) Sumita, J.; Shibata, T.; Nakagawa, S.; Iyoku, T.; Sawa, K. *J. Nucl. Sci. Technol.* **2009**, *46*, 690–698.
(39) Sham, T. K.; Naftel, S. J.; Coulthard, I. *Chemical Applications of Synchrotron Radiation*; World Scientific: Singapore, 2002; Vol. II.
(40) Sham, T. K. *Int. J. Nanotechnol.* **2008**, *5*, 1194–1246.
(41) Stöhr, J. *NEXAFS Spectroscopy*; Springer-Verlag: Berlin, Heidelberg, Germany, 1992.
(42) Rosenberg, R. A.; Love, P. J.; Rehn, V. *Phys. Rev. B* **1986**, *33*, 4034–4037.
(43) Hemraj-Benny, T.; Banerjee, S.; Sambasivan, S.; Balasubramanian, M.; Fischer, D. A.; Eres, G.; Puretzky, A. A.; Geohegan, D. B.; Lowndes, D. H.; Han, W.; Misewich, J. A.; Wong, S. S. *Small* **2006**, *2*, 26–35.
(44) Braun, A.; Huggins, F. E.; Shah, N.; Chen, Y.; Wirick, S.; Mun, S. B.; Jacobsen, C.; Huffman, G. P. *Carbon* **2005**, *43*, 117–124.
(45) Braun, A.; Kubatova, A.; Wirick, S.; Mun, S. B. *J. Electron Spectrosc. Relat. Phenom.* **2009**, *170*, 42–48.
(46) Yang, M. X.; Xi, M.; Yuan, H.; Bent, B. E.; Stevens, P.; White, J. M. *Surf. Sci.* **1995**, *341*, 9–18.
(47) Burchell, T.; Bratton, R.; Windes, W. *NGNP Graphite Selection and Acquisition Strategy*; Report ORNL/TM-2007/153; National Technical Information Service: Springfield, Virginia, United States of America, 2007.
(48) Zhou, X.; Wang, H.; Yu, S. *Nucl. Eng. Des.* **2011**, *241*, 752–754.
(49) Shibata, T.; Kunimoto, E.; Eto, M.; Shiozawa, S.; Sawa, K.; Oku, T.; Maruyama, T. *J. Nucl. Sci. Technol.* **2010**, *47*, 591–598.
(50) Plashkevych, O.; Yang, L.; Vahtras, O.; Ågren, H.; Pettersson, L. G. M. *Chem. Phys.* **1997**, *222*, 125–137.
(51) Vijayalakshmi, S.; Föhlisch, A.; Kirchmann, P. S.; Hennies, F.; Pietzsch, A.; Nagasono, M.; Wurth, W. *Surf. Sci.* **2006**, *600*, 4972–4977.
(52) Hitchcock, A. P.; Fischer, P.; Gedarken, A.; Robin, M. B. *J. Phys. Chem.* **1987**, *91*, 531–540.
(53) Brzhezinskaya, M. M.; Muradyan, V. E.; Vinogradov, N. A.; Preobrajenski, A. B.; Gudat, W.; Vinogradov, A. S. *Phys. Rev. B* **2009**, *79*, 155439/1–12.
(54) Genzer, J.; Sivaniah, E.; Kramer, E. J.; Wang, J.; Körner, H.; Xiang, M.-L.; Yang, S.; Ober, C. K.; Char, K.; Chaudhury, M. K.; Dekoven, B. M.; Bubeck, R. A.; Fischer, D. A.; Sambasivan, S. *Mater. Res. Soc. Symp. Proc.* **1998**, *524*, 365–370.
(55) Ishibara, M.; Shibata, T.; Hanawa, S. Transactions of the 15th International Conference on Structural Mechanics in Reactor Technology (SMIRT-15), Seoul, Korea, August 15—20, 1999.
(56) Lane, J. A.; MacPherson, H. G.; Maslan, F. *Fluid Fuel Reactors*; Addison-Wesley Pub. Co.: Reading, Massachusetts, U.S.A., 1958.
(57) Regier, T.; Paulsen, J.; Wright, G.; Coulthard, I.; Tan, K. H.; Sham, T. K.; Blyth, R. I. R. Synchrotron Radiation Instrumentation: Ninth International Conference on Synchrotron Radiation Instrumentation, AIP CP, Daegu, Korea, May 28-June 2, 2006.